STUDY OF DIFFERENCES BETWEEN SUNSPOT AREA DATA DETERMINED FROM GROUND-BASED AND SPACE-BORNE OBSERVATIONS

L. Győri[1], T. Baranyi[2], M. Turmon[3], and J.M. Pap[4]

[1]*Heliophysical Observatory, Gyula Observing Station, 5701 Gyula, P.O. Box 93, Hungary*
[2]*Heliophysical Observatory, 4010 Debrecen, P.O. Box 30, Hungary*
[3]*Jet Propulsion Laboratory, M/S 126-347, Pasadena, CA, 91109, USA*
[4]*Goddard Earth Sciences and Technology Center, University of Maryland Baltimore County, Greenbelt, USA*

ABSTRACT

The determination of the area of sunspots is important from several points of view, eg., in study of the evolution of sunspots and their effect on solar irradiance. Automated sunspot area measurements are now replacing time-consuming and subjective hand-made measurements. Also, terrestrial solar observations have been supplemented by observations from space. The resolution of the ground observations is limited by the seeing, while space-borne observations are limited by the size of the CCD array. The use of different data sources, as well as of different region identification algorithms, causes discrepancies in reported sunspot areas. An important task is to determine to what extent these differences can be attributed to different analysis methods and to what extent to different data. It is also important to establish the required spatial resolution of space-based images.

INTRODUCTION

Sunspots are the most easily observable features of the solar photosphere, while at the same time they are important manifestations of solar activity. Because of their importance, they have long been observed and measured on white-light full-disk solar images in several ground based observatories. Starting in 1996, space observations by the Michelson Doppler Imager (MDI) on SOHO (Scherrer et al., 1995) have also become available. One of the most important parameters of sunpots is their area, which is used directly or as a proxy in many fields of investigation. Precise area measurements are especially important in studies of irradiance variations; for example, Fröhlich et al. (1994) found that one of the largest obstacles in irradiance modeling is the incorrect measurement of sunspot area. However, area data obtained with different observation and analysis methods suffer from substantial systematic differences (e.g. Hoyt et al., 1983; Chapman et al., 1989; Steinegger et al., 1996; Baranyi et al., 2001). In order to take into account (or reduce) these differences, first of all one should reveal their causes. This paper examines the differences between the ground-based and space-borne images analyzed by the same image processing method.

DATA SOURCES

In a previous paper (Győri et al., 2002) we compared sunspot areas derived from different solar images using different image processing methods. One of the results of this comparison is shown in Figure 1(a). Here we applied the same image processing software SAM (Sunspot Automatic Measurement) to different solar images, namely to full-disk images obtained by MDI and ground-based photoheliograms. We found that sunspot areas derived from MDI images were about 13% larger than those derived from ground-based photoheliograms. Since the image processing method is the same in both cases, the found area difference should be related to the ways the MDI and the DPD (Debrecen Photoheliographic Data) images are taken.

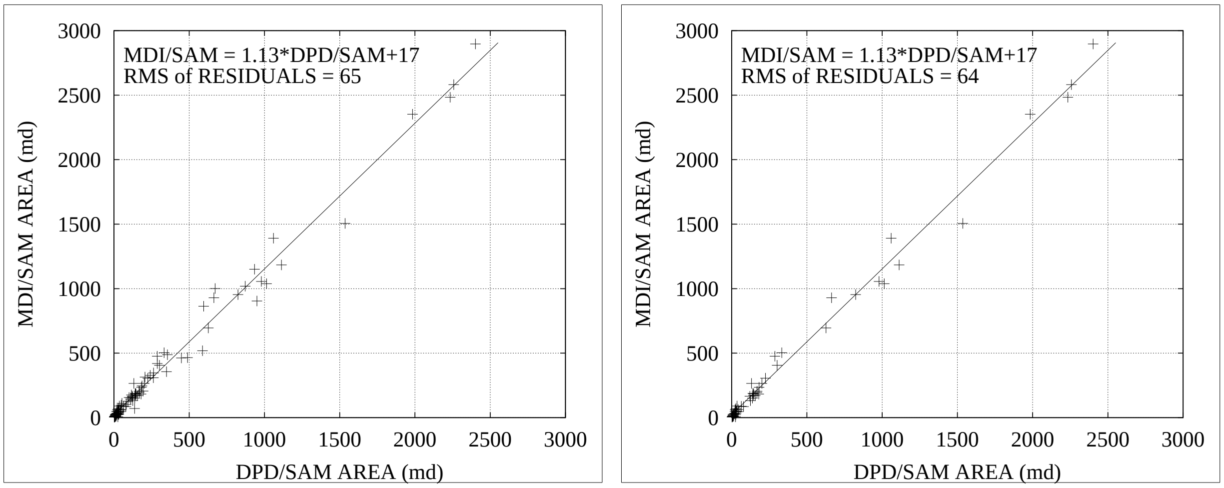

(a) Between $0^\circ - 90^\circ$ central meridian longitudes. (b) Between $0^\circ - 40^\circ$ central meridian longitudes.

Fig. 1. Projected sunspot areas in millionths of the solar disk determined by SAM from DPD photoheliograms versus from MDI images.

DPD Images

The DPD images are photoheliograms. The Gyula Observing Station (GOS) is the main contributor to the DPD catalogue; gaps are filled from collaborating observatories. For simplicity, we only deal with photoheliograms from GOS in this paper. The resolution of these images is confined by the diameter of the objective of the telescope and seeing conditions. The diameter of objective is 15 cm but it is stopped down to 10 cm because, according to our experience, this is the diameter that adapts the heliograph best to the prevailing seeing conditions. The heliograph contains an interference filter of 10 nm effective half-width centered at 554 nm. From these data the Rayleigh criterion for the resolution of the GOS objective is 1.4 arcses. But, for sources of nearly equal brightness, the superimposed Airy disks will appear non-circular for separation of about one third of Rayleigh's criterion (Kitchin, 1984). So, during excellent seeing, GOS can in principle achieve about 0.5 arcsec resolution. Gyula is a small town, and GOS is sited atop a massive water tower 44m above a grassy park. Due to its smooth grassy environment, its height, and the short exposure time of the photoheligrams, the seeing conditions for solar observations are rather good here. We estimate that the average seeing is between 1" and 2" but there are moments when the seeing is better than 1". The best of several photoheliograms taken during the day is used for the DPD. An SBIG ST7 16 bit/pixel CCD camera is used to digitize the photoheliogram. The plate scale of the CCD image is 0.3 arcsec/pixel.

MDI Images

The MDI intensity images are created by combining five narrowband filtergrams, hence they are sometimes described as quasi-continuum images. These images are taken by MDI with a CCD camera near the Ni I 676.8 nm absorption line originating in the mid-photosphere (Scherrer et al., 1995). We use the level 1.5 MDI imagery, which has been further preprocessed at JPL to remove several sources of spurious spatial and temporal variation (Turmon et al., 2002). An image-wide scale factor accounts for exposure-time jitter and varying instrument throughput; limb darkening is removed by a radial correction, adjusted for the slight ellipticity introduced by the MDI optics; leakage of the Doppler signal into the intensity proxy is eliminated by a velocity-dependent scaling; and finally a residual flat-field is removed. For the purposes of this analysis, these corrections are about equivalent to those used to produce the level 2.0 MDI data product. Their plate scale is about 2 arcsec per pixel.

SUNSPOT AREA ANALYSIS

There are three salient differences between the DPD and the full-disk MDI images: (1) the DPD images suffer from seeing; (2) the MDI images have lower resolution; (3) the MDI images are not continuum images. We demonstrate below that deficiencies in seeing may not cause the 13% difference observed in sunspot areas, and suggest that it is the rather lower resolution of the MDI images which adversely influences the sunspot area measurements.

Seeing Effects on Sunspot Area

As the DPD images are taken through the Earth's atmosphere, one could try to explain the sunspot area differences between DPD and MDI by arguing that due to seeing some small spots are overlooked in the DPD images while being present in the MDI images. Moreover, it is possible that poor seeing could in fact decrease the area of all sunspots, causing the DPD sunspot areas to become smaller. Three considerations lead us to reject these arguments.

First, we compare the sunspot images in Figure 2(a) and Figure 2(b). These two images were taken only 17 minutes apart. The DPD image was taken during average seeing conditions. It is evident that this DPD

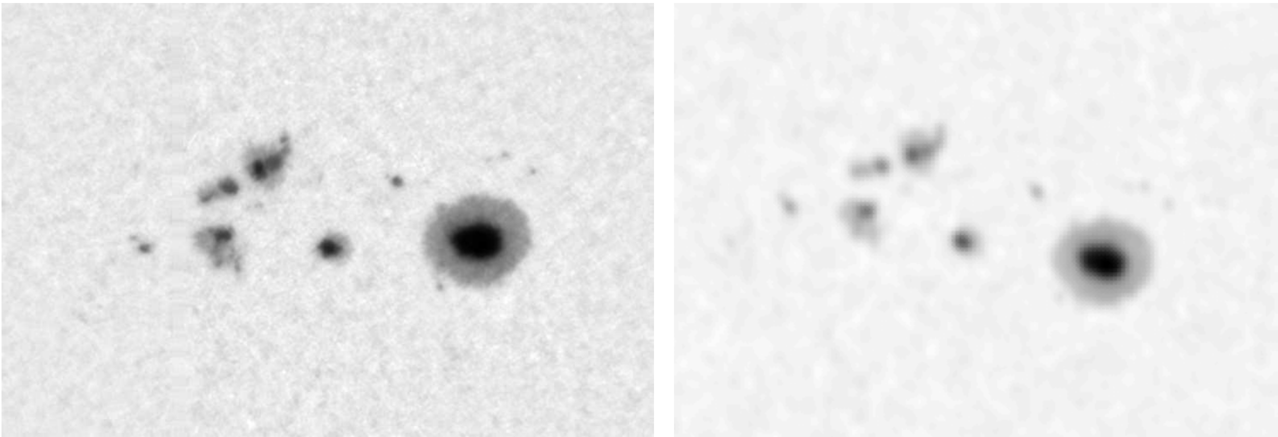

(a) DPD photoheliogram observed in Debrecen at 14:31 UT.

(b) MDI quasi-continuum image observed at 14:48 UT.

Fig. 2. Two images of active region NOAA 7981 on 1996 Aug. 2 taken within 17 minutes.

image contains more detail than the MDI image. For example, the small sunspot below and to the right of the main spot is clearly visible in the DPD image but has almost vanished from the MDI image, and the small pair at the left edge of the DPD image appears merged in the MDI image. Similar results are seen in other MDI/DPD comparisons; this is fully to be expected from the specifics of the telescopes. We conclude that under typical seeing conditions the small spots are not overlooked in the DPD image (at least relative to the MDI image).

Second, another way that seeing can influence the area measurement from the DPD image is through the so-called *visibility loss*, which we define as follows. Due to symmetry, the average total sunspot area should be the same (within statistical fluctuation) on the Sun for all longitude bands measured from the central meridian over a suitably long period of the time (e.g., one year during the solar maximum). But in fact, the average corrected total sunspot area steadily decreases from the central meridian to the limb (Hoyt et al., 1983). This phenomenon, the visibility loss, can be ascribed to three interplaying effects: the decreasing intensity contrast of the photosphere, decreasing resolution (relative to the solar surface) of the solar image, and the seeing interfering with the previous two as one goes from the center to the limb.

Figure 3 shows the total corrected sunspot areas in 10° longitude bands measured from the central meridian using sunspot areas from DPD for the years 1988, 1989, 1993, 1994, 1995, and 1996. Beyond 40° from the central meridian we can observe a steadily decreasing total corrected sunspot area due to visibility loss. In the band nearest the limb, the total corrected sunspot area is about 85% less than in the central bands. This is a bookkeeping artifact due to the movement of part of the sunspot group to the other side of the Sun.

If DPD areas do suffer from a seeing-induced visibility loss, it will become more pronounced at the limb. To examine how the visibility loss at the limb influences the area discrepancy between the two image types, we confine the area comparison to sunspot groups within 40° of the central meridian (see Figure 1(b)). Comparing Figure 1(a) and Figure 1(b) we see no sign of difference between them. The parameter of the regression line does not change either if the groups between 40°-90° central meridian longitudes are considerd. Thus we conclude that the smaller DPD areas can not, in this context, be ascribed to the visibility loss due to seeing. This last fact might indicate that the visibility loss at the limb can be attributed mainly to the decreased intensity contrast of the photosphere and not to seeing — so it is present in both DPD and MDI photograms.

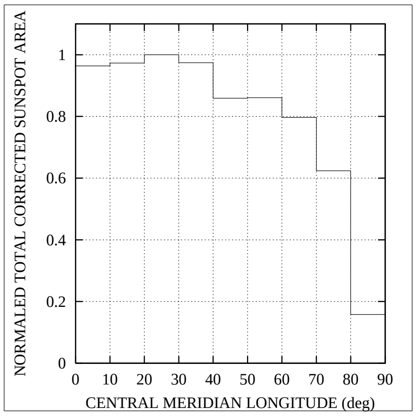

Fig. 3. The normalized total corrected DPD sunspot areas plotted in 10° central meridian longitude belts for 1988, 1989, 1993, 1994, 1995, and 1996.

Third, Steinegger et al. (1997), in their investigation of the effect of seeing on computed area, find that for inflexion-point based methods, sunspot area is essentially invariant to seeing parameters. (The small dependence they do find is that poor seeing slightly increases area.) The method they used to determine the effect of the seeing on the area of sunspots is as follows. At first they determined the sunspot area on a high resolution image (0.062" pixel^{-1}). Then they degraded the image by different seeing parameters and determined the sunspot area on the blurred images. One of the sunspot area determination procedures they used in this way is their inflexion point method (IMF). The results they obtained with IMF show that sunspot areas are very stable with respect to seeing in the blurring range they considered (0"–3"). As its name indicates, IMF gets information about the border of a sunspot using the steepest intensity gradient in the photogram. SAM is based on the same idea. Thus, both of the methods use basically the same information from the image. So the effect of the seeing on the the two methods should be the same. From this point of view, the sunspot areas determined by SAM on the DPD photoheliograms are not essentially influenced by the seeing.

Resolution Effects on Sunspot Area

As we exclude the causes that could make the DPD areas smaller due to seeing we conclude that it is the MDI sunspot areas which are larger than the real ones. We think that the larger MDI areas are a

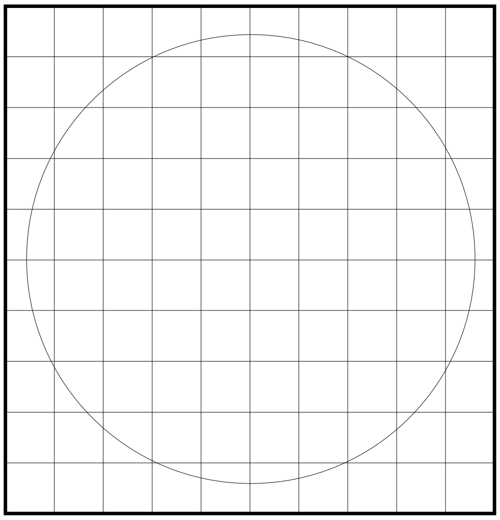

Fig. 4. A circular sunspot on the CCD matrix.

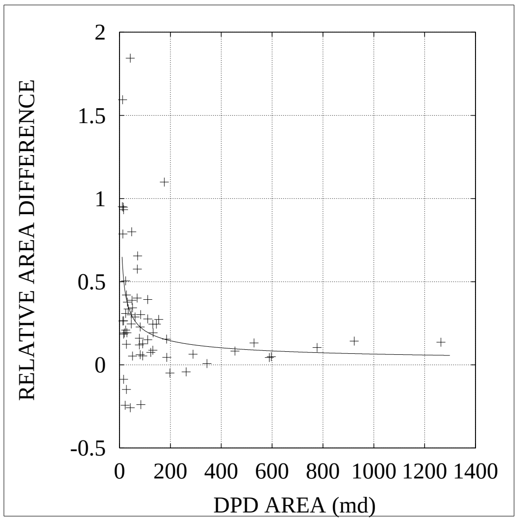

Fig. 5. Relative sunspot area difference versus DPD sunspot area. The continuous line is the function described by equation 2.

consequence of the lower resolution (2" plate scale) of the MDI continuum images. In fact, from Figure 4 we can see that there are many pixels which are covered only partly by the sunspot. Due to the typically high contrast of sunspot regions, even partial coverage will tend to depress intensity enough to result in a declaration of sunspot. In the area calculation, these partly covered pixels are counted as whole pixels which causes exaggerated sunspot areas.

It is expected intuitively that in the case of a round sunspot, the measured area can be calculated as if the radius of the spot were too large by about half of a pixel. The relative area difference (the area difference dA divided by the area A) of two circles with radius r and $r + dr$ is, to first order,

$$\frac{dA}{A} = \frac{2\,dr}{r} \quad . \tag{1}$$

If we express A in millionths of the solar disk (μd), then equation 1 becomes

$$\frac{dA}{A} = \frac{2000}{r_\odot}\frac{dr}{\sqrt{A}} \quad , \tag{2}$$

where $r_\odot$ is the radius of the solar disk, measured in the same units as dr. (The equations of course refer to individual sunspot areas.) We can try to verify equation 2 using DPD and MDI areas. Figure 5 shows the relative area differences of the sunspots measured on the DPD and the MDI images and the curve described by equation 1 with $dr = 0.5$ pixel (1" on the MDI images). Spot radius was determined from the area of the spot. To compile the figure we selected DPD and MDI images within 80 minutes to decrease the scatter originating from temporal differences between the two observations. Areas in Figure 5 are that of individual sunspots identified on both images. The fit of the curve given by equation 2 to the measured data is pretty much as expected indicating that the larger MDI/SAM areas can be explained by the lower plate scale of the MDI images.

We have observed phenomena related to equation 2 in several cases when selecting the individual sunspots from the MDI and DPD images for Figure 5. We found in several cases that stand-alone sunspots within a DPD image seemed inside a common penumbra on the corresponding MDI image. This occurred even when the observation times were so close that it was improbable that the spots really merged. Of course, the consequence of this resolution-induced merging is that the area of the combined spot is larger than the sum of the individual DPD spots.

CONCLUSIONS

We have given evidence that sunspot areas derived from MDI images are larger than the true ones due to the relatively small plate scale. The relative area difference between the MDI sunspot areas and the true ones can be described by equation 2. The relative error decreases as $1/\sqrt{A}$ with increasing area but the absolute error increases as $\sqrt{A}$ with increasing area.

However, it remains possible that another source of difference between these areas lies in the way these images are taken. Because the MDI images are averaged from five slices of the continuum, there could be a nonlinear relation between the two "intensity" observables. A nonlinearity would yield different results in an inflection-point based sunspot identification method applied to the two images. The resulting tendency to push the sunspot boundaries inward or outward would appear similar to that shown in Figure 5. This issue is under investigation.

We highlight a consequence of equation 2. If we reduce the linear size of a CCD pixel, the relative error in the sunspot area will decrease by the square of the reduction. For example, reducing the linear size of a pixel by half (doubling the linear size of the CCD array) reduces the relative error by a factor of four. Larger space-borne CCD arrays are clearly needed to increase the accuracy of sunspot area measurements from space.

ACKNOWLEDGMENTS

SOHO is a mission of international cooperation between ESA and NASA. The authors gratefully acknowledge the past and ongoing effort of the VIRGO and MDI teams. This research was supported by grants NAG5-10876 and NAG5-11624 from the SOHO Office of NASA's Office of Space Science as well as by a grant OTKA T037725 from Hungarian National Foundation for Scientific Research. The research described in this paper was carried out in part for the Jet Propulsion Laboratory, California Institute of Technology, under a contract with NASA.

REFERENCES

Baranyi T., L. Győri L., A. Ludmány, and H.E. Coffey, Comparison of sunspot area data bases, *MNRAS*, **323**, 223-230, 2001.

Chapman, G.A., A.D. Herzog, D.E. Laico et al., Photometric measurements of solar irradiance variations due to sunspots, *Astrophys. J.*, **343**, 547-553, 1989.

Fröhlich ,C., Pap J.M., and H.S. Hudson, Improvement of the Photometric Sunspot Index and changes of the disk-integrated sunspot contrast with time, *Solar Phys.*, **152**, 111-118, 1994.

Győri, L., Automation of area measurement of sunspots, *Solar Phys.*, **171**, 109-130, 1998.

Győri, L., T. Baranyi, M. Turmon, and J. M. Pap, Comparison of image-processing methods to extract solar features, *Proc. SOHO 11 Symp., ESA SP-508*, 203-208, 2002.

Hoyt, D. V., J. A. Eddy, and H. S. Hudson, Sunspot areas and solar irradiance variations during 1980, *Astrophys. J.*, **275**, 878-888, 1983.

Kitchin, C. R., *Astrophysical Techniques*, Adam Hilger Ltd, 40-41, Bristol, 1984.

Scherrer, P.H., R.S. Bogart, R.I. Bush et al., The solar oscillations investigation- Michelson Doppler Imager, *Solar Phys.*, **162**, 129-188, 1995.

Steinegger, M., M. Vázquez, J. A. Bonet, and P. N. Brandt, On the energy balance of solar active regions, *Astrophys. J.*, **461**, 478-498, 1996.

Steinegger, M., J. A. Bonet, and M. Vázquez, Simulation of seeing influences on the photometric determination of sunspots areas, *Solar Phys.*, **171**, 303-330, 1997.

Turmon, M., J.M. Pap, and S. Mukhtar, Statistical pattern recognition for labeling solar active regions: Application to SoHO/MDI imagery, *Astrophys. J.*, **568**, 396-407, 2002.

E-mail address of L. Győri ls@bekesnet.hu